Dissecting the molecular mechanism by which NH₂htau and Aβ1-42 peptides impair mitochondrial ANT-1 in Alzheimer disease

CrossMark

A. Bobba [a], G. Amadoro [b], V.A. Petragallo [a], P. Calissano [c], A. Atlante [a],*

[a] Institute of Biomembranes and Bioenergetics, CNR, Bari, Italy
[b] Institute of Translational Pharmacology, CNR, Rome, Italy
[c] European Brain Research Institute (EBRI), Rome, Italy

ARTICLE INFO

ABSTRACT

To find out whether and how the adenine nucleotide translocator-1 (ANT-1) inhibition due to NH₂htau and Aβ1-42 is due to an interplay between these two Alzheimer's peptides, ROS and ANT-1 thiols, use was made of mersalyl, a reversible alkylating agent of thiol groups that are oriented toward the external hydrophilic phase, to selectively block and protect, in a reversible manner, the –SH groups of ANT-1. The rate of ATP appearance outside mitochondria was measured as the increase in NADPH absorbance which occurs, following external addition of ADP, when ATP is produced by oxidative phosphorylation and exported from mitochondria in the presence of glucose, hexokinase and glucose-6-phosphate dehydrogenase. We found that the mitochondrial superoxide anions, whose production is induced at the level of Complex I by externally added Aβ1-42 and whose release from mitochondria is significantly reduced by the addition of the VDAC inhibitor DIDS, modify the thiol group/s present at the active site of mitochondrial ANT-1, impair ANT-1 in a mersalyl-prevented manner and abrogate the toxic effect of NH₂htau on ANT-1 when Aβ1-42 is already present. A molecular mechanism is proposed in which the pathological Aβ-NH₂htau interplay on ANT-1 in Alzheimer's neurons involves the thiol redox state of ANT-1 and the Aβ1-42-induced ROS increase. This result represents an important innovation because it suggests the possibility of using various strategies to protect cells at the mitochondrial level, by stabilizing or restoring mitochondrial function or by interfering with the energy metabolism providing a promising tool for treating or preventing AD.

© 2013 Elsevier B.V. All rights reserved.

1. Introduction

The histopathological characteristics of Alzheimer's disease (AD) are amyloid-β (Aβ) containing plaques and neurofibrillary tangles (NFTs) as well as neuronal and synaptic loss [1]. The underlying mechanisms of the interplay of plaques and tangles have remained essentially unresolved. Moreover, studies in several amyloid precursor protein and tau transgenic mouse models suggest that a possible link between these two characteristic AD hallmarks might be an early mitochondrial dysfunction, particularly at synapses, associated with increased oxidative stress [2–8]. The impairment of mitochondrial oxidative phosphorylation (OXPHOS), proportional both to cholinergic defects [9] and to clinical disability [10], has been extensively documented in the brain of AD patients [11]. Studies from molecular, cellular, animal models and postmortem brains have consistently revealed a causative role of mitochondrial dysfunction in AD synapse failure [12–15].

Recently, we have shown that a neurotoxic NH₂-tau fragment of the human tau40 isoform (441 amino acids), but not the physiological full-length protein, preferentially interacts with Aβ peptide(s) in human AD synapses in association with mitochondrial adenine nucleotide translocator-1 (ANT-1). Two Alzheimer's peptides – Aβ1-42 and the smaller and more potent Tau peptide NH₂-26-44 (NH₂htau), the minimal active moiety of longest overexpressed NH₂-26-230 human tau fragment(s) [16] – inhibit the ANT-1 in a non-competitive and competitive manner, respectively, and together further aggravate mitochondrial dysfunction by exacerbating ANT-1 impairment, thus leading to dysfunction in energy metabolism prior to induction of cell death [16–18].

In this paper we dissect the molecular mechanism by which NH₂-htau and Aβ1-42 impair mitochondrial ANT-1. Since it is known that ANT contains –SH groups, which are both essential for the catalytic activity and preferential targets for reactive oxygen species (ROS) attack, we have investigated whether the ANT-1 inhibition is due to

an interplay between these two Alzheimer's peptides, ROS and ANT-1 thiols. To accomplish this purpose we turned to mersalyl (MERS), a reversible alkylating agent of thiol groups that are oriented toward the external hydrophilic phase [19], to selectively block and protect the –SH groups of ANT-1 in a reversible manner.

The ability of Aβ1-42 to induce mitochondrial ROS production and of mersalyl to protect ANT-1 against truncated NH_2htau, but not Aβ1-42, were observed.

2. Materials and methods

2.1. Ethics statements

This study was performed in accordance with the local ethics committee and with the principles contained in the Helsinki Declaration, as revised in 1996. All animals were handled and cared for in accordance with EEC guidelines (Directive 86/609/CEE).

2.2. Reagents

Synthetic NH_2htau peptides were synthesized by Sigma Genosys (Haverhill, UK) and purified to >95% homogeneity by reversed-phase high pressure liquid chromatography on C-18 silica columns with monitoring of A_{214} (peptide bonds).

Aβ1-42 and the inverse sequence peptide, Aβ42-1, (Sigma Chemicals Co., St. Louis, MO, USA) were prepared according to Eckert et al. [5] with minor modifications. The peptides were dissolved in deionized water at a concentration of 0.5 mM and stored at −20 °C. At occurrence, the peptide stock solution was diluted in phosphate buffer saline medium (PBS) to a concentration of 0.1 mM and incubated at 37 °C, with gentle agitation, for 24 h to obtain aged, aggregated preparations of peptide.

2.3. Cell culture and treatments

Primary cultures of cerebellar granule cells (CGCs) were obtained from 7-day-old Wistar rats as described by Levi et al. [20]. Cells were plated in basal medium Eagle (Invitrogen, Gibco) supplemented with 10% fetal calf serum, 25 mM KCl, 2 mM glutamine, and 100 μg/mL gentamicin on dishes coated with poly-L-lysine. Arabinofuranosylcytosine (10 μM) was added to the culture medium 18 to 22 h after plating to prevent proliferation of non neuronal cells.

2.4. Cell homogenate preparation

Cultured medium was removed and the plated CGCs were washed with PBS, containing 138 mM NaCl, 2.7 mM KCl, 8 mM Na_2HPO_4, and 15 mM KH_2PO_4, pH 7.4. Cell integrity was quantitatively assessed by the inability of cells to oxidize externally added succinate, and by the ability of ouabain to block glucose transport. Homogenates were prepared from a cell suspension by 10 strokes with a Dounce homogenizer at room temperature. Cytosolic lactate dehydrogenase was released and subsequent treatment with Triton-X-100 did not cause further release. Consistently with Atlante et al. [21], homogenate, containing mitochondria, was checked both for the mitochondrial coupling efficiency by measuring both the respiratory control index (RCI), *i.e.* (oxygen uptake rate after adenosine diphosphate [ADP] addition) / (oxygen uptake rate before ADP addition), which reflects the ability of mitochondria to produce adenosine triphosphate (ATP), and the generation of membrane potential (Δψ), monitored by the decrease of safranine O absorbance at 520 nm, and for the intactness of the mitochondrial membranes, by measuring in the postmitochondrial supernatant the activities of adenylate kinase (ADK, E.C.2.7.4.3) and glutamate dehydrogenase (GDH, E.C.1.4.1.3), which are marker enzymes of the mitochondrial intermembrane space and matrix, respectively. Protein content was determined

according to Waddell and Hill [22] with bovine serum albumin used as a standard.

2.5. Polarographic measurements

O_2 consumption was measured polarographically by means of a Gilson 5/6 oxygraph using a Clark electrode see [21]. The cell homogenate in PBS (about 0.2 mg protein) was incubated in a thermostated (25 °C) water-jacketed glass vessel (final volume equal to 1.5 ml), and polarographic measurements were performed in the presence of 1 mM ADP or 0.1 μM FCCP. The substrate used was β-hydroxybutyrate (β-OH, 5 mM). Instrument sensitivity was such as to allow rates of O_2 uptake as low as 0.5 natom min^{-1} mg^{-1} protein to be followed.

2.6. ANT-1-mediated ADP/ATP exchange measurements

Cell homogenates (0.1 mg protein), containing mitochondria, were incubated at 25 °C in 2 ml of standard medium consisting of 200 mM sucrose, 10 mM KCl, 1 mM $MgCl_2$, and 20 mM HEPES–Tris, pH 7.2. The appearance of ATP in the extramitochondrial phase, due to externally added ADP, was assayed, as in Atlante et al. [17,21], by using the ATP detecting system (ATP D.S.) consisting of glucose (2.5 mM), hexokinase (HK, 0.5 e.u.), glucose-6-phosphate dehydrogenase (G-6-PDH, 0.5 e.u.), and $NADP^+$ (0.2 mM) in the presence of 10 μM P_1,P_5-Di(adenosine-5')pentaphosphate (Ap$_5$A), a specific inhibitor of adenylate kinase. The coupled enzymatic system used to detect ATP outside mitochondria was proved not to be rate limiting *per se* since while the addition of 5 μM ATP resulted in an increase in the rate of absorbance, no rate increase occurred following the addition of both substrate and enzyme components of the ATP detecting system. Similarly it has always been verified that the $NADP^+$ reduction was a measure of the ADP/ATP exchange rate, via ANT-1 (see Results).

Furthermore, control experiments were carried out in the presence of either atractyloside (ATR) or oligomycin (OLIGO) to ensure that both the ADP/ATP exchange was mediated by the ADP/ATP carrier and no substrate-level phosphorylation occurs, respectively [17,21]. Worthy of note is the uniqueness of this model, in which mitochondria are both intact and coupled thus providing a 'physiological' environment for the investigation of ANT-1 *in situ*.

The rate of $NADP^+$ reduction, which is the measure of the ADP/ATP exchange via ANT-1, in the extramitochondrial phase was determined following the absorbance increase at 340 nm, measured as the tangent to the initial part of the progress curve and expressed as nmoles $NADP^+$ reduced / minute × mg cell protein.

2.7. Superoxide anion detection

$O_2^{-\bullet}$ was detected according to the Fe^{3+}-cyt *c* method [23,24] and by using the MitoSox dye (for refs see [25,26]). In the Fe^{3+}-cyt *c* method, cell homogenate in PBS (about 0.2 mg of protein/2 ml) was incubated at 25 °C in the presence of Fe^{3+}-cyt *c* (10 μM) plus a mitochondrial respiratory substrate, such as succinate (5 mM), under experimental condition in which succinate-driven ROS generation is largely due to the reverse electron transport (RET) (see [27–30] and references therein).

The increase in absorbance at 550 nm, *i.e.* Fe^{2+}-cyt *c* formation ($\varepsilon_{550} = 31.7$ mM^{-1} cm^{-1}), was measured using a PerkinElmer LS-5 spectrophotometer equipped with a thermostated holder. A calibration curve is made by using an $O_2^{-\bullet}$-producing system, *i.e.* xanthine (XX) + xanthine oxidase (XOD).

To specifically detect superoxide anion production of mitochondrial origin use was made of MitoSOX Red, a specific mitochondrial dye – highly and exclusively sensitive to superoxide [25,26], but not to other reactive oxygen/nitrogen species – which is selectively targeted to mitochondria where it accumulates as a function of mitochondrial

membrane potential and exhibits fluorescence upon oxidation by superoxide and subsequent binding to mitochondrial DNA. Cell homogenate in PBS was preincubated with succinate (10 mM) plus ADP (2.5 mM) for 2 min at 25 °C. After addition of 1 μM MitoSOX red and further 15 min incubation, fluorescence emission at 580 nm was measured using a Perkin-Elmer LS-50B Luminescence Spectrofluorimeter. Fluorescence spectra (λex = 396 nm; λem range: 500–700 nm) were recorded under the same experimental conditions.

2.8. Statistical analysis

Experiments were carried out in triplicate and repeated at least 3 times. Data are expressed as means ± standard deviation (S.D.) ($n > 3$). Difference between control and treated groups were analyzed with SPSS software by 1-way analysis of variance (ANOVA) for repeated measures followed by the *post-hoc* Bonferroni test for multiple comparisons. Statistical differences were determined at $p < 0.05$. Experimental plots were obtained using Grafit (Erithacus Software).

3. Results

The ADP/ATP carrier, that mediates the exchange transport of ADP and ATP in mitochondria, is essential for the synthesis of ATP by oxidative phosphorylation which supplies bioenergy for various biochemical reactions. Furthermore we have recently demonstrated that NH$_2$htau and Aβ1-42 impair mitochondrial ANT-1 [17,18].

Taking into account that the ANT contains four –SH groups involved in the transport activity [31,32], which are also known to be the main targets of ROS [33,34] and with the aim to investigate the mechanism of inhibition exerted by the AD peptides on the ANT activity, essential studies were performed to ascertain: *i)* whether ANT-1 activity was affected either by mersalyl or by ROS-producing system; *ii)* whether there was any interaction between the carrier thiol/s and ROS; and *iii)* whether and how the interaction of NH$_2$htau and Aβ1-42 with ANT-1 involves carrier thiol/s.

First, to illustrate at present the state of the art on this topic, a comprehensive scheme on the effect of the AD peptides on ANT-1 together with kinetic characteristics, relevant references and the novelty use of Aβ42-1 in this paper, is reported in Table 1.

3.1. Effects of either mersalyl or ROS-producing system on ANT-1 activity

To determine whether and how ANT-1-mediated ADP/ATP exchange was affected by either mersalyl (Fig. 1) or ROS-producing

Table 1
Effect of Alzheimer's peptides on ANT-1.

Peptide	ANT-1				
	V	p	Inhibition Nature	Ki	Refs.
No peptide	10.0 ± 0.8	-	-	-	21
Aβ1-42	7.0 ± 0.5	< 0.05	Non Competitive	2 μM	18
Aβ42-1	9.5 ± 0.6	> 0.05	No	-	this paper
NH$_2$26-44 tau	1.8 ± 0.3	<0.01	Competitive	0.1 μM	17-18
NH$_2$1-25 tau	9.7 ± 0.5	> 0.05	No	-	17

All the peptides – Aβ 1-42, Aβ 42-1, NH$_2$-26-44, *i.e.* NH$_2$htau, and NH$_2$-1-25 – were added at a final concentration of 1 μM. ANT-1 is measured following the appearance of ATP, due to ADP (0.1 mM) addition to CGC homogenates (0.1 mg protein), and monitored photometrically at 340 nm (for details see Materials and methods (2.6 *section*) and refs. [17,18,21]).
V indicates the rate values – expressed as nmoles NADP$_+$ reduced/min x mg protein – means ± SD from five experiments carried out using different cell preparations. Statistical analysis was by ANOVA and Bonferroni test: $p < 0.05$, $p < 0.01$ when all the samples were compared with the control, *i.e.* no peptide. When $p > 0.05$: differences are not statistically significant.

system, *i.e.* XX + XOD (Fig. 2), the rate of supply in the cytosol of ATP, produced by OXPHOS, was continuously measured by using a kinetic approach already used and validated in our previous papers [17,21]. Since this unique experimental model strictly requires that mitochondria are intact and coupled to provide a 'physiological' environment for the investigation of ANT *in situ*, before starting each experiments, cell homogenate was routinely checked for both the functional integrity of mitochondria and the generation of membrane potential (see Materials and methods, Sections 2.4 and 2.5 respectively).

In a typical experiment, the homogenate, treated with AP$_5$A (10 μM) to inhibit adenylate kinase (for ref see [21]) and to prevent mitochondrial ATP synthesis in a manner not dependent on OXPHOS, was incubated in the presence of an ATP detecting system (ATP D.S.) (see Materials and methods, Section 2.6). The ATP concentration in the extramitochondrial phase of the homogenates was negligible as shown by the fact that no increase in the absorbance measured at 340 nm was found in the presence of glucose, hexokinase, glucose-6-phosphate dehydrogenase and NADP$^+$. As a result of ADP addition (0.1 mM), an increase in the NADPH absorbance was observed, indicating the appearance of ATP in the extramitochondrial phase. The rate of NADPH formation was approximately 10 nmol NADP$^+$ reduced/min mg cell protein (Fig. 1A, trace *a*), in good agreement with values obtained by Atlante et al. [17,21]. NADPH formation derives from *i)* ADP uptake into mitochondria in exchange for endogenous ATP, *ii)* ATP synthesis from imported ADP via ATP synthase and *iii)* efflux of the newly synthesized ATP from the mitochondria in exchange for further ADP via ANT-1. It should be noted that under the experimental conditions used the oxidation of endogenous substrates is sufficient to supply energy for ATP synthesis.

As expected, NADPH formation was completely inhibited by the presence of oligomycin (OLIGO, 10 μM), the classical inhibitor of ATP synthase, further confirming that no ATP could be synthesized via substrate-level phosphorylation in the homogenates (Fig. 1B, traces a). The addition of ATR (10 μM), an impermeable ANT inhibitor, also strongly inhibited NADPH formation, as expected in light of the Ki value (about 3 μM) see [21] and of the ADP and ATR concentrations used. Because the ANT-1-mediated ADP/ATP exchange could depend on a number of events, including electron flow across the mitochondrial membrane, electrochemical proton gradient generation, ATP synthase and the adenine nucleotide content of the mitochondria, we investigated the rate-limiting step of the process leading to ATP efflux from the mitochondria. Then, to gain some insight into the residual ability of the mitochondria to drive ATP synthesis by generating $\Delta\psi$ and to ascertain whether this could limit the rate of ATP production, we energized cell homogenates with β-hydroxybutyrate, a respiratory substrate that enters mitochondria via diffusion with an increase in $\Delta\psi$ (see Fig. 1B, traces b). The rate of ATP production was not significantly increased but addition of a cocktail of the electron flow inhibitors, *i.e.* rotenone, antimycin and mixothiazole (RAM) plus cyanide (CN$^-$), totally prevented ATP production, thus confirming both that available energy is not limiting the process and that the process depends exclusively on the oxidation of endogenous substrates. Furthermore, also inorganic phosphate (Pi), which is known to enter the mitochondria using its own carrier and to be necessary for ATP synthesis, when added to the homogenate did not influence the ADP/ATP exchange rate, thus proving that endogenous Pi is sufficient and not limiting for the process (Fig. 1B, traces b).

To definitely confirm that the method here employed, *i.e.* measurement of the rate of NADPH formation, exclusively measures the rate of ADP/ATP exchange in mitochondria [17,21], we applied the control flux coefficient (control strength) criterion [35,36] for the plot data when either ATR or OLIGO was used as inhibitor at 0.1 mM ADP. As shown in Fig. 1C, the coincidence of the intercepts on the y axis of the lines fitting the points obtained in the presence of ATR, but not OLIGO, which – as known – inhibits ATP synthase,
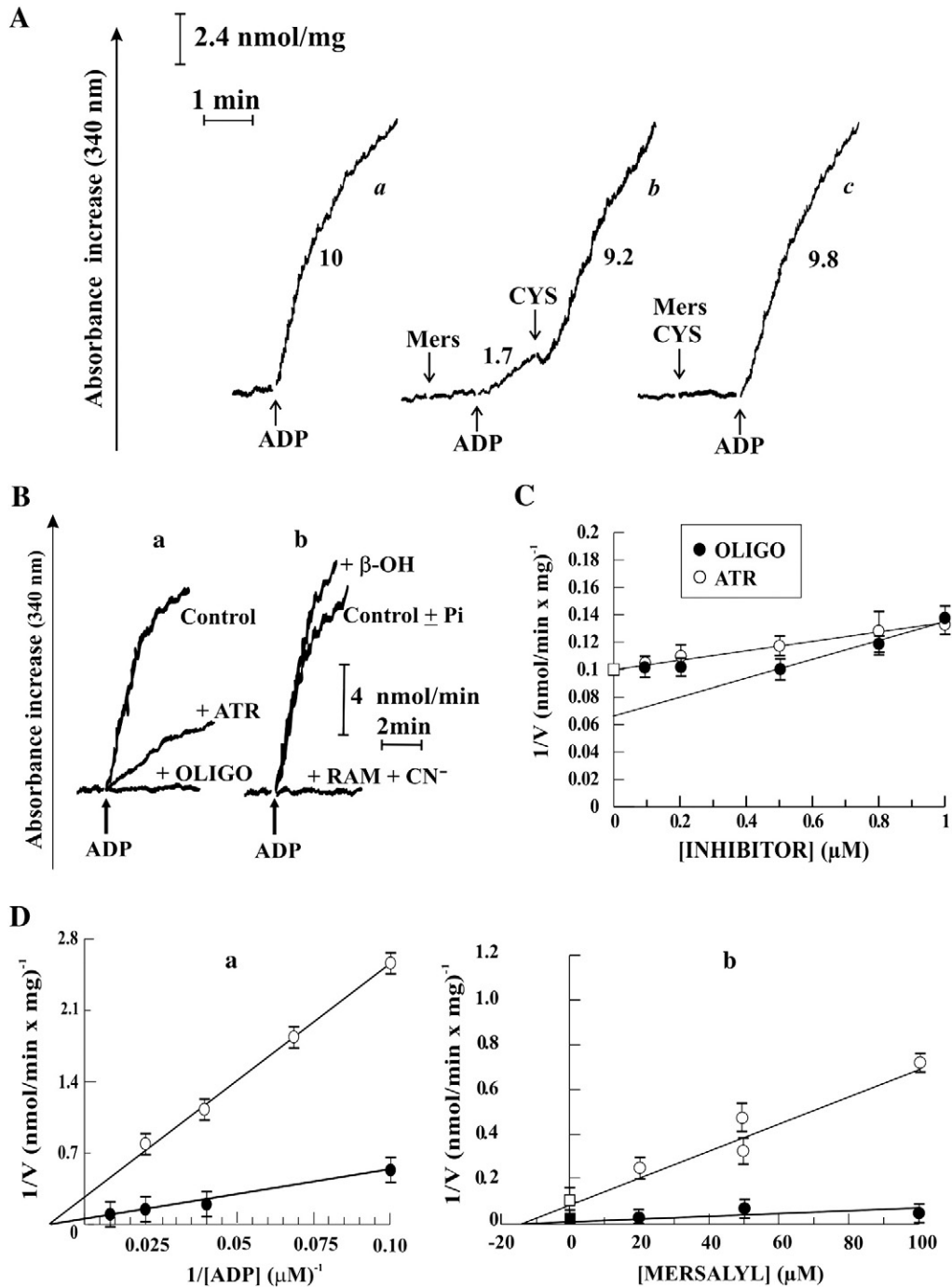
Fig. 1. Effects of mersalyl on ANT-1-dependent ADP/ATP exchange. A) Appearance of ATP, due to ADP (0.1 mM) addition to CGC homogenates (0.1 mg protein), was monitored photometrically at 340 nm, as described in the Materials and methods (2.6 section). Where indicated, additions were as follows: mersalyl (MERS, 0.05 mM), cysteine (CYS, 1 mM). The reaction was started by the addition of ADP at the time indicated by the arrow. For details see the text. B) Atractyloside (ATR, 10 μM), oligomycin (OLIGO, 10 μM), β-hydroxybutyrate (β-OH, 5 mM), inorganic phosphate (Pi, 1 mM), the cocktail of respiratory chain inhibitors (RAM), *i.e.* rotenone (3 μM), antimycin A (0.8 μM) and mixothiazole (6 μM), plus cyanide (CN⁻, 1 mM), were added to the reaction mixtures 1 min before ADP (0.1 mM). C) Dixon plot of the inhibition by either ATR or OLIGO, at the indicated concentrations, of the ADP/ATP exchange rate measured in CGC homogenate. The ADP concentration was 0.1 mM. Reported values are the mean of three independent neuronal preparations (with comparable results) each one in triplicate with the standard deviation. D) Experimental conditions as in the panel A. The plot of 1/v vs the reciprocal of external ADP concentration (a) was investigated in the absence (●) or presence of 0.05 mM Mersalyl (○) and the same data were replotted as 1/v vs the mersalyl concentration in a Dixon plot (b) using two different ADP concentrations: 0.1 mM (○) and 0.25 mM (●). Reported values are the mean of four independent neuronal preparations (with comparable results) each one in triplicate with standard deviation.

clearly shows that the rate of absorbance increase at 340 nm, due to NADPH formation, is indeed a measure of the ADP/ATP exchange.

When mersalyl (MERS, 50 μM) was added 1 min before ADP addition, the rate was strongly decreased to 1.7 nmol NADP⁺ reduced/min mg cell protein, thus confirming the sensitivity of ANT-1 –SH group/s to the thiol reagent (Fig. 1A, trace *b*). Addition of 1 mM

CYS, which reverse the reaction of MERS with functional thiols [37], almost completely restores the NADPH formation rate (about 9.2 nmol NADP⁺ reduced/min mg cell protein) (Fig. 1A, trace *b*). As expected, the simultaneous addition of CYS and MERS had no effect on ATP appearance in the extramitochondrial phase (9.8 nmol NADP⁺ reduced/min mg cell protein) thus confirming the ability of
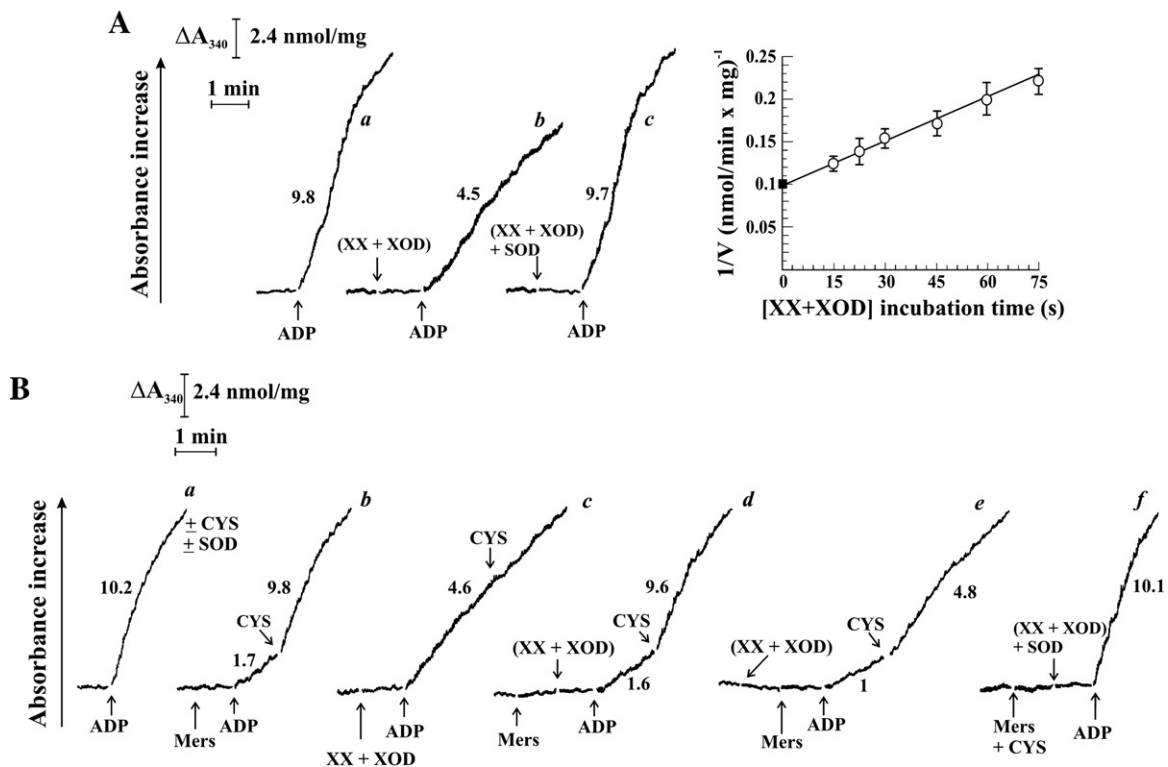
Fig. 2. Effects of ROS-producing system on ANT-1-dependent ADP/ATP exchange. A–B) Appearance of ATP, due to ADP (0.1 mM) addition to CGC homogenates (0.1 mg protein), was monitored photometrically at 340 nm, as reported in Fig. 1. Where indicated, additions were as follows: xanthine (XX, 10 μM) plus xanthine oxidase (XOD, 1 e.u./ml), superoxide dismutase (SOD, 5 e.u./ml), mersalyl (MERS, 0.05 mM), cysteine (CYS, 1 mM). The reaction was started by the addition of ADP at the time indicated by the arrow. For details see the text. In the *inset* to panel A: Experimental condition as in the panel. The Dixon plot of 1/absorbance increase rate *vs* the [XX + XOD]-incubation time, *i.e.* increased level of superoxide over time, was investigated by using 0.1 mM ADP. Reported values are the mean of three independent neuronal preparations (with comparable results) each one in triplicate with the standard deviation.

CYS to prevent the effect of mersalyl (Fig. 1A, trace *c*). The nature of the MERS inhibition was studied by investigating the dependence of the NADPH formation rate as a function of ADP concentration in cell homogenate in the absence or presence of the thiol reagent (Fig. 1Da). A purely non competitive inhibition was found with a Km value (*i.e.* the ADP concentration which gives half-maximum rate of exchange) equal to 40 μM, and a Ki value (*i.e.* the concentration of MERS which gives 50% inhibition) equal to 15 μM.

When the experimental data of Fig. 1Da were replotted as 1/v *vs* the MERS concentration in a Dixon plot (Fig. 1Db), straight lines were obtained. Statistical analysis shows that the intercepts to the ordinate axis, obtained by treating the experimental points according to linear regression, coincide perfectly with the corresponding experimental controls, *i.e.* in the absence of mersalyl. This clearly shows not only that the measured inhibition is related to the same parameter measured in the control, *i.e.* the rate of ADP/ATP exchange, but has also the additional value of ruling out a possible inhibitory effect by mersalyl on ATP synthase or other proteins having CYS residues, in agreement with [17,18,21]. Moreover, appropriate controls were carried out to exclude that the observed inhibition was due to the effect of mersalyl on the ATP detection system.

Next, in order to confirm that ANT-1 is target of ROS, as already observed in CGCs undergoing apoptosis in which ROS level increases [38], we carried out another set of experiments in which ANT-1-mediated ADP/ATP exchange was monitored in the presence of an artificial ROS generation system, *i.e.* the XX plus XOD, according to [39] (Fig. 2A). A decrease in the ANT-1 transport efficiency occurs (*trace b*, 4.5 nmol NADP⁺ reduced/min mg cell protein), likely due to –SH groups oxidation, which is completely prevented by superoxide dismutase (SOD) (*trace c*, 9.7 nmol NADP⁺ reduced/min mg cell protein).

By applying again the control strength criterion we verified that XX/XOD-dependent ROS production inhibits ANT-1, but not ATPase

(see inset to Fig. 2A). Also in this case, in fact, the intercepts to the *y axis*, obtained by treating the experimental points according to linear regression, coincides perfectly with the corresponding experimental controls, *i.e.* in the absence of XX/XOD system. In order to eliminate any doubt, the lack of inhibition by XX + XOD on ATP synthase activity was also confirmed by measuring both the FCCP-stimulated swelling of mersalyl-treated mitochondria incubated with ATP (for ref see [17]) and the oligomycin-sensitive ATP hydrolase activity of Complex V according to [40] (data not shown).

Fig. 2B shows an experimental strategy developed to study the capability of MERS to protect ANT-1 thiols from ROS attack. By analyzing traces *a–f* step by step, it is clear that, as already seen above (Fig. 1), a strong inhibition of the rate of NADPH formation was observed in the presence of MERS which is reversed by CYS (comparing *a* with *b*). However, the 55% inhibition observed in the presence of (XX + XOD) (comparing *a* with *c*) is not reversed by CYS. When (XX + XOD) system was added after MERS addition, the rates measured both before and after CYS addition were no different from the control, *i.e.* in the absence of ROS producing system (comparing *b* and *d*). On the contrary, no complete CYS reversal was observed when the (XX + XOD) system was added before MERS (*e*): in this case the rate, obtained after CYS addition, is quite similar to that of *trace c*. As a control, it was verified that no inhibition occurred if both MERS + CYS and (XX + XOD) + SOD were added before starting the reaction with ADP (*f*). The protection by mersalyl against ROS attack strongly suggested that the ANT-1 impairment derives from the action exerted by ROS on targets which are apparently sensitive to mersalyl, *i.e.* –SH group(s) (for refs see [32]). No effect by mersalyl on XOD + XX-dependent superoxide formation was observed under the same experimental conditions used in the figure (not shown).

In the light of the crucial role played by the ADP/ATP carrier in OXPHOS, the effect of mersalyl or a ROS-producing system on oxygen

consumption, *i.e.* mitochondrial respiration, was investigated in order to confirm that the inhibition of ANT-1 likely involves its own thiol group(s). The effect of mersalyl or ROS was investigated on *State 3/ Uncoupled respiration* in which oxygen uptake is stimulated either by addition of ADP or by using an uncoupler, such as FCCP, respectively (Fig. 3A). The difference is that in the former case the stimulation of oxygen uptake derives from ADP used to drive ATP synthesis, whereas in the latter case it derives from FCCP-dependent collapse of the electrochemical proton gradient without ATP synthesis. Mitochondria from cell homogenate in *State 4*, *i.e.* in the presence of β-hydroxy-butyrrate (βOH) alone, a respiratory substrate which enters mitochondria via diffusion – thus ruling out the possibility that a membrane translocator of an energetic substrate, for example the dicarboxylate carrier which transport succinate into mitochondria, can limit the overall process of oxygen consumption – took up oxygen at a rate of 12 natom O_2/min mg cell protein. When ADP was added, the rate increased up to 63 natom O_2/min mg cell protein with an RCI value equal to 5.2 (*trace a*). In the presence of either MERS (*trace b*) or the (XX + XOD) system (*trace c*), added 1 min before βOH, the rate enhancement due to ADP phosphorylation was strongly reduced. But, when CYS or SOD was added simultaneously with either MERS or the ROS-producing system, the ADP rate increase was recovered (*traces d* and *e,* respectively). On the other hand, the addition of FCCP increased the rate of oxygen uptake up to 98 natom O_2/min mg cell protein (*trace a′*) with an Uncoupling Control Ratio (UCR, the ratio of the rate of oxygen uptake in uncoupled respiration and *State 4*) equal to 8. No change in the rate of oxygen uptake occurred when either MERS or (XX + XOD) was added separately either before (*traces b′* and *c′,* respectively) or after the respiratory substrate (not shown), further confirming that the electron flow along the respiratory chain is not affected by either of the compounds. Statistical analysis of the experimental data, carried out in triplicate and repeated 3 times, reported in Fig. 3B, confirms that
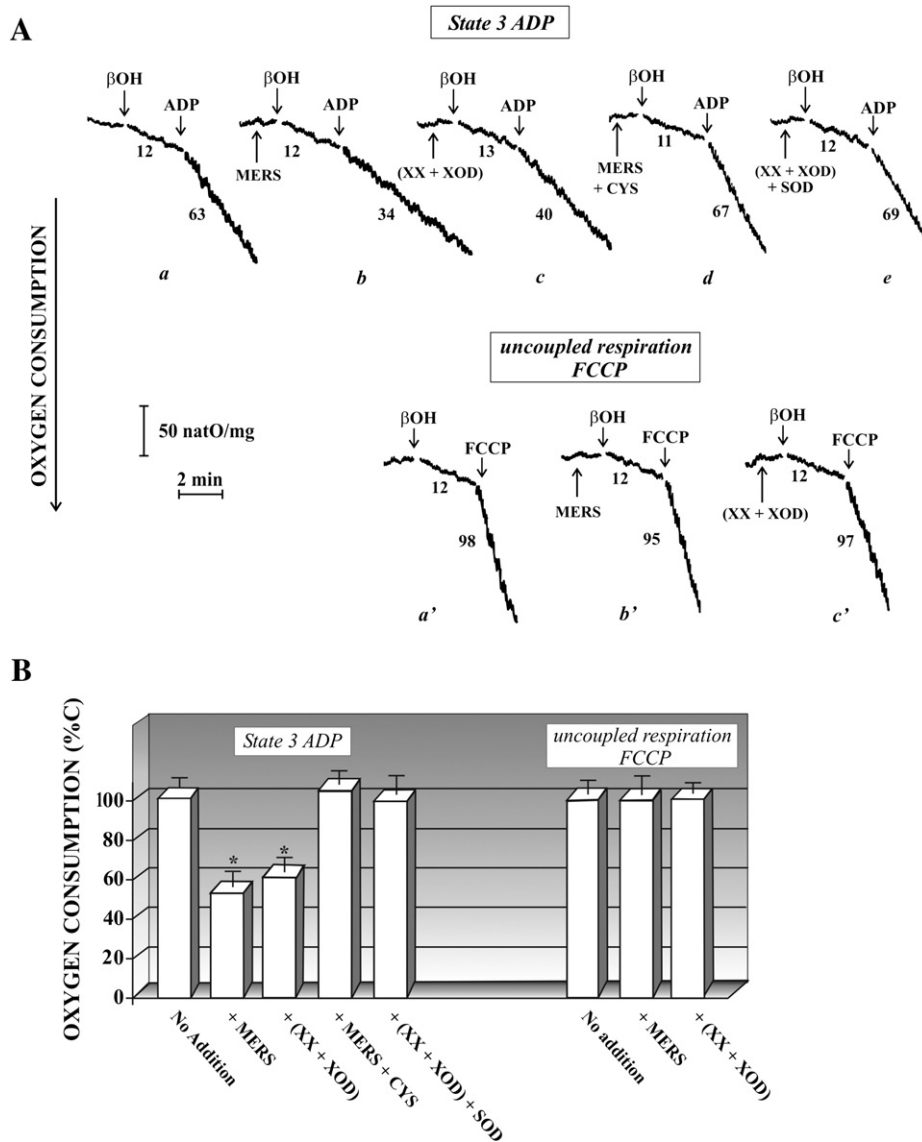

Fig. 3. Effects of either mersalyl or a ROS-producing system on ADP/FCCP-stimulated mitochondrial respiration (state 3/uncoupled respiration) by CGC homogenate due to β-hydroxybutyrate. A) CGC homogenate (0.1 mg cell protein) was suspended in standard medium at 25 °C in a water-jacketed glass vessel and consumption of O_2 was monitored polarographically. β-hydroxybutyrate (β-OH, 5 mM), ADP (1 mM), FCCP 0.1 μM were added at the indicated times. Mersalyl (MERS, 0.1 mM), cysteine (CYS, 1 mM), xanthine (XX, 10 μM) plus xanthine oxidase (XOD, 1 e.u./ml), superoxide dismutase (SOD, 5 e.u./ml), when present, were added 1 min before β-OH addition. They had no effect on *state 4* of respiration, *i.e.* in the absence of ADP. Rates of oxygen uptake were expressed as natom O_2/min mg cell protein. B) Sample prepared as described in A). The rates of oxygen uptake were expressed as % of control sample, *i.e.* no addition. A value of 100% is given to the oxygen consumption rate value after ADP addition for state 3_{ADP} or after FCCP addition *uncoupled respiration*$_{FCCP}$. Reported values are the mean of three independent neuronal preparations (with comparable results) each one in triplicate with the standard deviation. Statistical analysis was by ANOVA and the Bonferroni test. For the *state 3*$_{ADP}$: *$p < 0.01$ when oxygen consumption in the presence of either MERS or (XX + XOD) was compared with sample in absence of any addition.

the decrease in oxygen consumption induced by either MERS or XX + XOD after ADP addition is statistically significant (*$p < 0.01$ with respect to control).

3.2. Aβ triggers mitochondrial increase of ROS production

Mitochondrial dysfunction has been identified in sporadic and familial AD cases [41,42] as well as in AD mouse model [43] in part due to elevated Aβ-induced oxidative stress. Since the mitochondrial respiratory chain (RC) is the major source of ROS in most cells [44], in a first set of experiment we verified whether Aβ1-42 is able to induce mitochondrial production of ROS when added to the CGC homogenate (Fig. 4). In order to do this, two methodological approaches were adopted: the Fe^{3+}-cyt c method, already used in our previous studies [23,38,45], and another method, sensitive only to superoxide of mitochondrial origin, which utilizes MitoSOX, a fluorogenic dye that selectively targets mitochondria.

In a typical experiment, when cell homogenate in PBS was incubated in the presence of Fe^{3+}-cyt c and the mitochondrial respiratory substrate succinate (SUCC, 5 mM), no absorbance increase at 550 nm due to reduction of Fe^{3+}-cyt c was observed, i.e. negligible ROS production was revealed (Fig. 4A, traces a). On the other hand, a

progressive increase in superoxide anion production was found in the presence of Aβ1-42 at concentrations ranging from 0.5 to 5 μM (Fig. 4A, traces b) which is completely prevented by the antioxidant SOD (Fig. 4A, traces c). Moreover, the absorbance signal in the Aβ1-42-treated homogenate was completely suppressed in the presence of the uncoupler FCCP (Fig. 4B, traces a) and the voltage-dependent anion channel blocker DIDS (Fig. 4B, traces b) indicating that [Aβ]-dependent superoxide production is predominantly mediated by mitochondria and that Aβ directly participates in the onset of oxidative stress in AD. As a control, no absorbance increase at 550 nm (i.e. no superoxide formation) was measured in the absence or presence of either Aβ or cell homogenate (data not shown).

That the succinate-driven ROS generation is largely due to RET, consistently with [27–30,46], is proved by the almost complete inhibition of the superoxide production rate by the Complex I blocker rotenone (Fig. 4B, traces c). Taking into account that notwithstanding in vivo the major reducing equivalent that supports the respiratory chain is NADH, and that both forward and reverse electron fluxes along the respiratory chain are linked to superoxide formation in vitro, the residual activity observed with SUCC in the presence of rotenone can be likely attributed to the combined superoxide generation by Complex II and Complex III (see [47]). Consistently, we
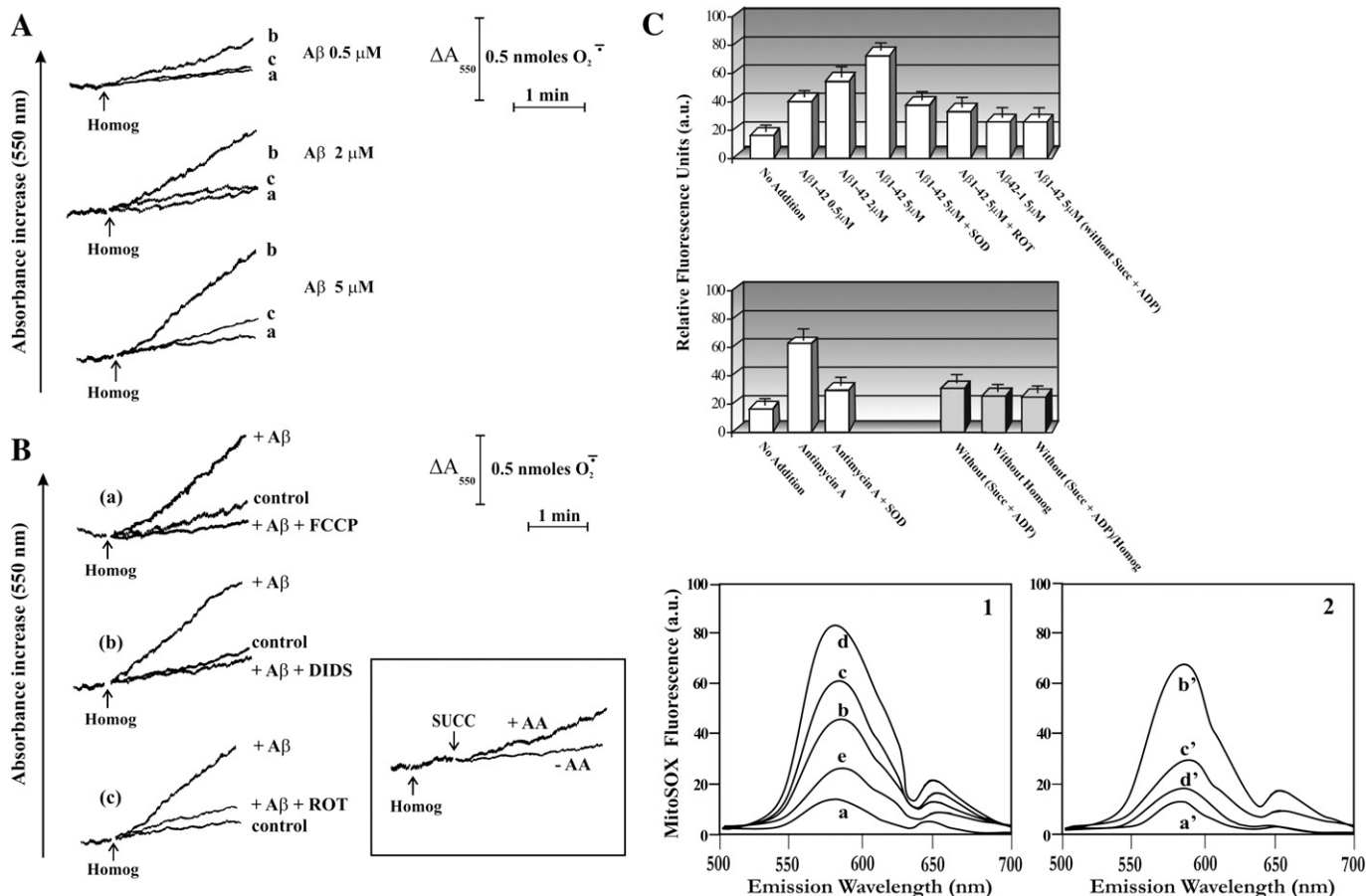

Fig. 4. Aβ-dependent ROS production by CGC homogenate. A) ROS production was started by the addition of homogenate (0.2 mg protein/ml) to PBS added with 10 μM Fe^{3+}-cyt c, 5 mM succinate in the absence (traces a) or presence of Aβ1-42 at 3 different concentrations (traces b): 0.5, 2 and 5 μM. Superoxide dismutase (SOD, 5 e.u./ml) addition (traces c). The rate of Fe^{2+}-cyt c production, i.e. superoxide anion formation, was measured as the absorbance increase at 550 nm and expressed as nmol of O_2^- formed/min x mg protein. B) Experimental condition as in A). Aβ1-42 (5 μM) was added to PBS, either in the absence or presence of FCCP (0.1 μM) (a), DIDS (1 mM) (b) or rotenone (3 μM) (c). In the inset, as a control, superoxide production in homogenate oxidizing succinate was induced, under artificial condition, by antimycin A (0.15 μM) addition. C) Cell homogenate (0.2 mg protein/ml), preincubated with 10 mM succinate, 2.5 mM ADP (or as indicated) for 2 min, was added with 1 μM MitoSOX with stirring at 25 °C. Fluorescence emission at 580 nm was recorded 15 min after Aβ (0.5–5 μM) or 5 μM Aβ42-1 or 0.15 μM Antimycin A (AA) addition. Where indicated SOD (5 U/ml) or Rotenone (ROT, 3 μM) were present. In the insets 1–2, fluorescence spectra (λex = 396 nm; λem range: 500–700 nm) were recorded under the same experimental conditions. Fluorescence intensity is reported in arbitrary units (a.u.). The experiment was repeated four times giving values with 5–10% variation. Inset 1: No addition (trace a), Aβ1-42 (0.5–2–5 μM) (traces b–c–d), Aβ1-42 (5 μM) + SOD (trace e). Inset 2: No addition (trace a′), AA (trace b′), AA + SOD (trace c′), 5 μM Aβ42-1 (trace d′).

verified (inset 1 to Fig. 4B) whether ROS are produced by Complex III, in the presence of SUCC, under artificial conditions in which this Complex is inhibited by antimycin A [48].

That the superoxide production observed in the presence of Aβ1-42 is indeed of mitochondrial origin was further confirmed by MitoSOX analysis. Cell homogenate (0.2 mg protein/ml) which contains respiring mitochondria in *State 3* (*i.e.* in the presence of 10 mM succinate plus 2.5 mM ADP) was incubated with 1 μM MitoSox with stirring at 25 °C. Mitochondrial $O_2^{-\bullet}$ production, measured as fluorescence intensity, increased progressively depending on Aβ1-42 concentrations (Fig. 4C) and was almost completely prevented by SOD and ROT in accordance with results of Fig. 4A and B. No MitoSox oxidation occurred when homogenate was incubated with the reverse sequence peptide Aβ42-1, nor when Aβ 1-42 was added to homogenate incubated with MitoSOX in the absence of SUCC + ADP. As a control, it was verified that fluorescence level increased in the presence of antimycin A (0.15 μM), added after 1 min to stimulate $O_2^{-\bullet}$ generation by Complex III, and this effect was reversed by SOD addition. As expected no $O_2^{-\bullet}$ formation, *i.e.* no fluorescence increase, was detected when MitoSox was added to *i)* homogenate in the absence of SUCC + ADP, *ii)* medium with SUCC + ADP but without homogenate, and *iii)* medium without both homogenate and SUCC + ADP.

In parallel experiment, emission fluorescence spectra, which exibit a peak close to 580 nm due to the $O_2^{-\bullet}$ dependent MitoSOX oxidation, were carried out, essentially as in [49,50]. As shown in the inset 1 to Fig. 4C, incubation of cell homogenate with Aβ1-42 used

at three different concentrations, induces a progressive increase of the fluorescence emission spectra (*traces b–c–d*) which is prevented by SOD (*trace e*). No fluorescence increase can be detected in the absence of Aβ (*trace a*). As a control, the same experiment carried out in the presence of antimycin A (inset 2 to Fig. 4C) showed an increase of the fluorescence emission peak at 580 nm (*trace b′*) – with respect to control (*trace a′*) – completely prevented by SOD (*trace c′*). As expected, Aβ 42-1 doesn't induce any increase in fluorescence (*trace d′*). Worthy of note is that, besides Aβ42-1, also NH₂htau does not produce superoxide anion under the same experimental condition (not shown), in agreement with [17].

3.3. ROS-mediated interaction between Aβ1-42, NH₂htau and ANT-1

In our previous reports [17,18] we have demonstrated that *i)* the two AD peptides, Aβ 1-42 and NH₂htau individually impaired the ANT-1 activity; *ii)* they further aggravate the mitochondrial dysfunction when added together, by exacerbating the ANT-1 impairment and emphasizing a synergistic effect in perishing mitochondria; and *iii)* Aβ1-42, added first to cell homogenate, was able to decrease the inhibitory effect of NH₂htau on ANT-1 activity.

Thus, in the light of the finding that Aβ1-42 but not NH₂htau or Aβ42-1, induces an increase of mitochondrial ROS (Fig. 4), we investigated whether SOD, added together with Aβ and before the addition of NH₂htau, is able to modulate/prevent the inhibitory effect of NH₂-htau on ANT-1. To do this, pre-treatment of cell homogenate with either Aβ1-42, at a concentration equal to its Ki value, *i.e.* 2 μM, or

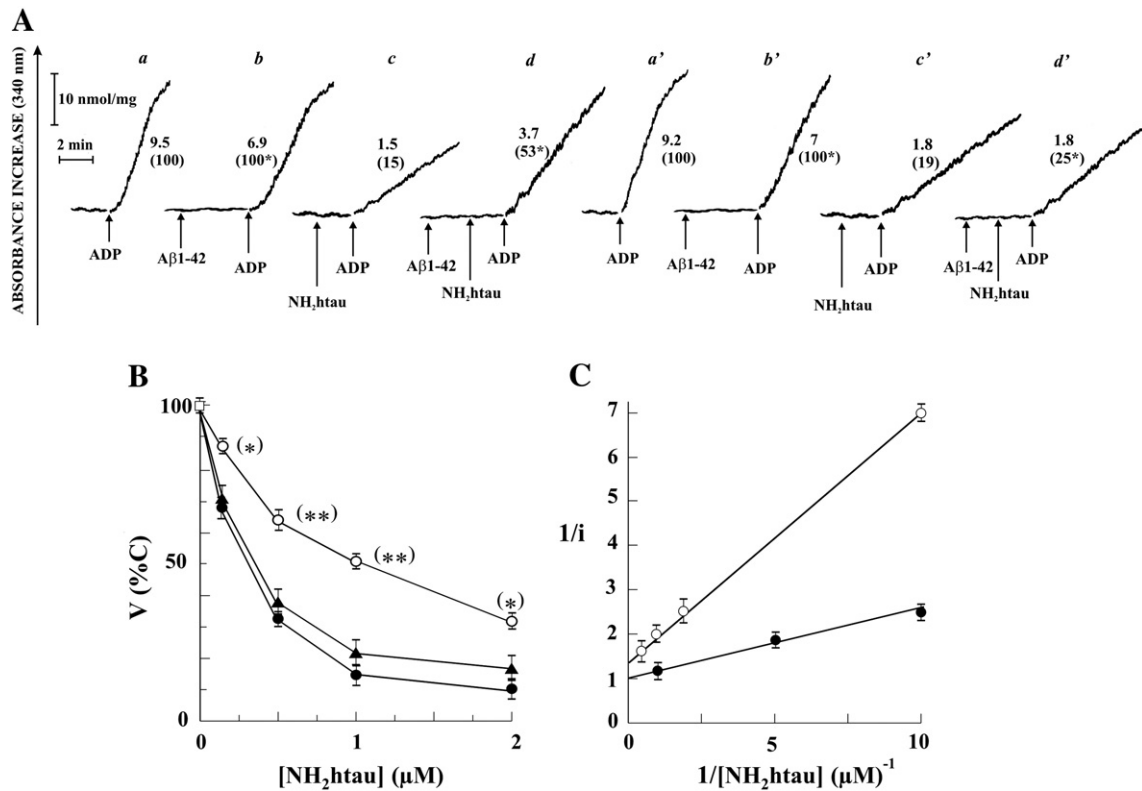**Fig. 5.** SOD prevents the Aβ1-42-induced lowering level of inhibition by NH₂htau on ANT-1. Experimental conditions as in Fig. 1. In A *(a–d)*: Aβ1-42, at concentration equal to its Ki value, *i.e.*, 2 μM, was incubated with homogenate 2 min before NH₂htau (1 μM). The reaction was started with ADP (0.1 mM) addition at the time indicated by the arrow. In A *(a′–d′)*: the same experimental conditions with the exception of the presence of superoxide dismutase (SOD, 5 e.u./ml) in the medium. The rate is expressed as nmol NADP⁺ reduced/minute per mg cell protein. The % rate value is reported in brackets. The value (100) is given to ADP reaction, *a)*; 100* is the value given to the ADP reaction in the presence of Aβ1-42, *b)*. In B: the dependence of ADP/ATP exchange rate, expressed as % C, in the absence (●) or presence of either Aβ1-42 (○) or Aβ1-42 plus SOD (▲), on the concentration of NH₂htau is reported. In C: data obtained in B were plotted as 1/i vs 1/[Inhibitor], with the fractional inhibition i = 1 − vi/vo (where vi and vo are the rates of ATP efflux in the presence or absence of the inhibitor, respectively). Values are mean ± SD from five experiments, carried out using different cell preparations. Statistical analysis was by ANOVA and the Bonferroni test: no statistically significant differences were found for the dependence of ADP/ATP exchange rate in the absence of Aβ1-42 (●) *versus* Aβ1-42 plus SOD (▲). *p < 0.01, **p < 0.001 for the dependence of ADP/ATP exchange rate in the absence of Aβ1-42 (●) *versus* Aβ1-42 (○).

NH$_2$htau (1 μM) for 4 or 2 min before ADP addition, respectively, induces a decrease in the rate of ATP appearance up to 6.9 and 1.5 nmol NADP$^+$ reduced/min mg cell protein, respectively, as compared to control (9.5 nmol NADP$^+$ reduced/min mg cell protein) (Fig. 5A, comparing a with b and c). No difference in the extent of inhibition of the rate of ATP appearance was observed in the presence of SOD (Fig. 5A, a′–c′). When Aβ1-42 was incubated with the cell homogenate for 2 min before NH$_2$htau (Fig. 5A, d), the rate of ATP appearance was partially recovered (3.7 nmol NADP$^+$ reduced/min mg cell protein) and the inhibition extent decreased up to 47% while it was 85% in the case of the NH$_2$htau added alone (comparing traces a and b with traces c and d), in good agreement with [18]. Surprisingly, the NH$_2$htau inhibitory effect on the ANT-1 was almost completely unaffected by Aβ1-42 (75 % inhibition vs 80%) if SOD was present (comparing trace d with d′).

In Fig. 5B the dependence of the rate (V, %C) of ATP appearance on the NH$_2$htau concentrations was investigated in the absence (●) and presence of Aβ1-42 (2 μM) either with (▲) or without SOD (○). As shown, the level of inhibition by NH$_2$htau, at various concentrations, lowered in the presence of Aβ1-42, was recovered if SOD was added together with Aβ, suggesting a mechanism of inhibition by NH$_2$htau which involves Aβ-mediated ROS production. To better investigate this aspect, we developed an experimental strategy that allowed us to solve the puzzle. Briefly, we investigated the effect of mersalyl, which – as shown above – is able to protect ANT-1 thiol/s from ROS attack (see Fig. 2), added before exposure of ANT-1 to the peptides, either added individually or together (Table 2). The mixture ANT-1-MERS plus peptide (i.e. NH$_2$htau or Aβ1-42 or NH$_2$htau plus Aβ1-42) was centrifuged in order to remove the supernatant containing the unbound peptide/s and the resulting pellet was used to follow the appearance of ATP due to ADP added after addition of CYS which detaches the MERS bound to SH group/s. As shown in Table 2, either NH$_2$htau (line 3) or Aβ1-42 (line 5) or both of them (line 7) were incubated with mitochondria for 3 min, after which i) centrifugation was performed, ii) the pellet was resuspended, iii) CYS was added and iv) NADPH formation was monitored after ADP addition. As expected, the reaction rate, expressed as % of the control to which value 100 (line 1) was given, was equal to 18, 74 and 12 for NH$_2$htau, Aβ1-42 and NH$_2$htau plus Aβ1-42 respectively and consistently with [18]. When MERS was added 1 min before the peptide, no NH$_2$htau inhibition was detected (comparing lines 2 and 4) (97 vs 98). On the contrary, about 25% inhibition was confirmed when either Aβ1-42 or NH$_2$htau + Aβ1-42 was/were added after MERS (lines 6 and 8, respectively). These findings suggest that the lack of the inhibitory effect of NH$_2$htau on ANT-1, which occurred when it was preceded by MERS, is likely due to a MERS-mediated protection of –SH group/s involved in the interaction of NH$_2$htau, but not of Aβ1-42 with ANT-1. The same applied to the effect of Aβ1-42 + NH$_2$htau (line 8), thus further confirming that the rate of NADPH synthesis was strictly dependent on the treatment of mitochondrial membrane with MERS, regardless of the interaction between Aβ and NH$_2$htau.

Now, in the light of our previous (see [18]) and new results in this paper, we considered that Aβ1-42 induces a decrease of the inhibitory effect by NH$_2$htau on ANT-1. To further confirm this point, data obtained in Fig. 5B were plotted as $1/i$ vs $1/[\text{Inhibitor}]$ (Fig. 5C), with the fractional inhibition $i = 1 - v_i/v_o$ (where v_i and v_o are the rates of ATP efflux in the presence or absence of the inhibitor, respectively). We observed that the intercepts on the y-axis of the line obtained by fitting the experimental points obtained in the presence of NH$_2$htau fragment alone was 1, showing that NH$_2$htau completely prevented ADP/ATP exchange. On the contrary, when Aβ1-42 was present, i.e. under conditions of decreased inhibitory effect by NH$_2$htau on ANT-1, the value on the y-axis intercept was not 1, this likely suggesting a protective effect of Aβ1-42 against NH$_2$htau toxicity within the cell.

Table 2
Protection by Mersalyl of ANT-1 thiol group/s from Aβ 1-42-produced ROS attack.

line	T = 0	T = 1'	T = 4'	CYS	ADP	V(%C)
1	–	–	Centrif	+ CYS	ADP	100
2	Mersalyl	–	Centrif	+ CYS	ADP	98
3	–	NH2hTau	Centrif	+ CYS	ADP	18**
4	Mersalyl	NH2hTau	Centrif	+ CYS	ADP	97
5	–	A-βeta	Centrif	+ CYS	ADP	74*
6	Mersalyl	A-βeta	Centrif	+ CYS	ADP	75§
7	–	A-βeta + NH2hTau	Centrif	+ CYS	ADP	12**
8	Mersalyl	A-βeta + NH2hTau	Centrif	+ CYS	ADP	73§

Rat cerebellar granule cell (CGC) homogenates (0.1 mg protein), containing mitochondria, were incubated at 25 °C. Either NH$_2$htau or Aβ1-42, at concentration equal to 1 and 2 μM respectively, was incubated with homogenate 1 min after MERS (50 μM) addition. At the time indicated in the table, the suspension was centrifuged and the pellet, resuspended in 2.0 ml of standard medium (see Materials and methods), was incubated with CYS (1 mM) and then with the ATP detection system. Appearance of ATP due to ADP (0.1 mM) addition was monitored as described in the Materials and methods. The value (100) is given to ADP reaction.
Values are mean ± SD from four experiments, carried out using different cell preparations.
Statistical analysis was by ANOVA and Bonferroni test: *$p < 0.01$, **$p < 0.001$ when compared all the samples (shaded lines) with each other; §$p < 0.01$ when compared all the samples (clear lines) with each other.

4. Discussion

We discuss here the close inter-relationship between the impairment of mitochondrial ANT-1 and the two main pathological features, i.e. plaques and NFTs, or Aβ and truncated tau peptides, which occur in the pathogenic process underlying AD [51]. Recently, we have proved that a neurotoxic NH$_2$-derived tau fragment mapping between 26 and 230 aa of the human tau40 isoform preferentially interacts with Aβ peptide(s) in human AD tissues in association with mitochondrial ANT-1 and Cyclophilin D. These two peptides, Aβ1-42 and NH$_2$htau fragment, but not NH$_2$1-25 [17] nor Aβ 42-1 (Table 1), inhibit ANT-1-dependent ADP/ATP exchange in a non-competitive and competitive manner, suggesting that mitochondrial dysfunction is triggered by ANT-1 impairment [18].

On the basis of these results to further investigate the process which modulates the interaction of the NH$_2$htau and Aβ1-42 peptides with ANT-1, we turned to an experimental model consisting of rat cerebellar granule homogenates (see Materials and methods, 2.4 section) added with AD peptides, in agreement with (see [18]), as the most appropriate and suitable experimental system to obtain information on both the target protein of Aβ1-42 and NH$_2$htau, i.e. mitochondrial ANT-1, and the interplay between the carrier protein and the AD peptides. As far as the concentration of synthetic AD peptides is concerned, the experimental 0.5–2 μM range, lower than the physiological neuronal concentration, was used as in (see [18]), thus mimicking an in vivo situation. The choice of CGCs as experimental model relies on the findings that during the onset of apoptosis of CGNs, several molecular events reminiscent of AD are induced such as activation of the amyloidogenic process, cleavage of tau and production of toxic fragments [see [52] and refs therein]. Furthermore emerging literature claims about a cerebellar involvement in AD and arguing definitively against the common practice of employing cerebellum as a negative control in biochemical studies [see [53] and refs therein].

We discuss first the involvement of the –SH group/s of ANT-1 in its activity to drive the export of ATP from the mitochondria in addition to the role as ROS target; second, the Aβ-induced mitochondrial extra-ROS production is briefly considered; finally attention is focused on the molecular mechanism through which thiol group/s modulate mitochondrial ANT-1 impairment in the presence of truncated NH$_2$tau and Aβ under increased ROS production conditions.

4.1. ROS-thiol/s interaction in the ANT-1 impairment and protection by mersalyl

In most mammalian cells, the major site of ATP synthesis is in the mitochondria, through OXPHOS, while the major use of ATP is in the cytosol and other intracellular organelles. Thus it is essential to have a rapid mechanism for transporting ATP out of the mitochondria and ADP back in. This is the major physiological role of ANT [54]. It is constituted of 297 amino acid residues and among them the four cysteines, *i.e.*, CYS56, CYS128, CYS159, and CYS256 [55] are well known target sites for thiol reagents such as eosin-5-maleimide, mersalyl, and N-ethylmaleimide [56,57]. Mersalyl can react with the –SH group in a reversible manner and this feature renders it suitable for performing studies on the involvement of –SH groups in the toxicity exerted by the two Alzheimer's proteins toward mitochondria. Notwithstanding mersalyl is an impermeable SH-reagent due to its charged nature, as a matter of clarity it should be considered that since both the ANT hydrophilic loop, containing CYS159, has been proposed to intrude the translocation channel into the membrane region, being accessible from the c-side [58,59], and the measurement of ANT activity performed in our manuscript reflects a dynamic situation in which the carrier molecule undergoes *c*- and *m*-state transition, somehow, during the re-orientation of the carrier within the membrane, this CYS residue could become transiently accessible to mersalyl added from the cytosolic side.

Indeed, the experimental observations reported in this paper show that the ANT-1 is strongly inhibited by mersalyl (Fig. 1), in agreement with [60–62]. Non-competitive inhibition was observed (Fig. 1) and, as expected, CYS was able to reverse/prevent the reaction of mersalyl with functional thiols [37] thus restoring the activity of the ANT-1. It should be noted that the use of other thiol reagents, such as N-ethyl-maleimide (NEM), was excluded because NEM gives an irreversible inhibition (not shown) (for refs see [55]).

This paper not only confirms that ROS, also those produced by an artificial system consisting of XX plus XOD, impair the ANT-1 in a mersalyl-prevented manner, but it has the added dimension of showing that thiol(s) in ANT-1 molecules is/are targets of ROS (Fig. 2A, B) [for refs. see [37,63,64], thus suggesting that a chemical modification in the carrier molecule is responsible for the change in ANT-1 activity. Our finding is consistent with the paper by Moreno et al. [65]: singlet oxygen, produced by irradiation of photosensitizer-loaded mitochondria, triggers permeability transition pore (PTP) opening and thiol reagents, in particular mersalyl, prevent the PTP opening when mitochondria are irradiated after addition of mersalyl. This is in agreement with the observation of Atlante et al. [66], according to which ANT is a major target of ROS-dependent photodynamic action.

4.2. Aβ 1-42 increases ROS production by the mitochondrial respiratory chain

It is now widely accepted that oxidative stress, manifested by protein oxidation, lipid peroxidation and mtDNA damage is a characteristic of AD brain [4,6,13] and Aβ1-42 has proved to induce oxidative stress in AD brain in a manner prevented by vitamin E [67], catalase or synthetic catalytic free radical scavenger [68,69]. Among the sources of ROS within a cell, mitochondria are the main producer of superoxide anion [44,64] and with the recent theory of RIRR (ROS Induced-ROS Release from mitochondria) [70] they have also a key role in determining ROS dynamics within a cell [71,72].

By using a method which measured the RET due to succinate addition and which is rotenone-sensitive [27–30], we demonstrated that external addition of Aβ1-42 to cell homogenate was able to induce ROS production likely at the level of Complex I. It should be noted that SUCC was used as an energy substrate under both the experimental conditions used, *i.e.* Fe^{3+}-cyt *c* and MitoSox, to emphasize more strongly that an increase of mitochondrial ROS production

occurs in the presence of Aβ see experiment of Fig. 4). Aβ dependent ROS extra-production still occurs in the presence of the sole endogenous mitochondrial substrates as shown in the experiments of Fig. 5 and Table 2 where energy substrate was not externally added.

On the other hand, Aβ1-42 did not induce production of ROS at Complex III, under the experimental conditions in Fig. 4. Consistent with this finding is the general opinion that the Complex I seems to be a more relevant location for Aβ-induced ROS formation, although the precise mechanism and the physiological and pathological conditions that promote the one-electron reduction of oxygen at this site require further clarification [73]. Nevertheless we cannot exclude at this time that other source of ROS may be involved. Anyway, further investigations are underway both to resolve this question and to investigate the effect of Aβ1-42 on mitochondrial respiration in a general context (*manuscript in preparation*).

4.3. Role of thiol redox state in modulating mitochondrial ANT-1 activity in the presence of NH₂htau and Aβ1-42

This study was undertaken with the aim of providing additional data on the possible participation of ANT-sulfhydryl groups in regulating ANT-1 activity in the presence of both NH₂htau and Aβ1-42. According to [74], here we show that ROS, produced by the mitochondrial RC, provide a redox signal which reversibly modifies the thiol redox state of mitochondrial ANT-1. Indeed, the reversible thiol redox modification of enzyme activity by ROS may be an important and unexplored mode of mitochondrial redox signaling. Some mitochondrial proteins have shown ROS-dependent thiol oxidation: peroxiredoxin III (PrxIII) [75], $NADP^+$-dependent isocitrate dehydrogenase [76], and Complex I [77,78].

In order to investigate the role of ANT–SH groups in regulating ANT-1 activity in the presence of pathological NH₂htau and Aβ1-42 and under conditions in which they are the target of ROS, strategic experiments were designed to determine whether specific protection by mersalyl could prevent the impairment of ANT-1 caused by NH₂htau and Aβ1-42 either added alone or together.

–SH group protection by mersalyl not only prevents the effect of NH₂htau, but not of Aβ1-42, on ANT-1 activity, but also abrogates the toxic effect of NH₂htau on ANT-1 when Aβ1-42 is already present. These results, and the previous ones [18], converge toward a picture, depicted in Scheme 1, in which NH₂htau inhibits ANT-1 in a MERS-prevented manner (panel A), while Aβ1-42 induces ROS production and interacts with ANT-1 in a non-competitive manner. Furthermore, Aβ1-42, added before the NH₂htau fragment, strongly reduces its ability to reach the ANT-1 active site and decreases its inhibitory action on mitochondrial function as a consequence of thiol group/s oxidation and conformational changes in the carrier protein (panel A'). In this regard it should be considered that, unlike Aβ, it is unknown whether or not the NH2-tau fragment enters mitochondria. Paradoxically, Aβ1-42 protects the cell from the inhibitory effect of NH₂htau on ANT-1 (see results reported in Table 2 together with the experiment reported in Fig. 5).

In this regard, we observed that also ADP, added to cultured CGCs, reduced the tau effectiveness in inhibiting ANT-1, like Aβ1-42 does (*manuscript in preparation*). It might be possible that binding of ADP to the carrier could grant protection against thiol oxidation by i) promoting alterations of the ADP/ATP carrier conformation that change the position of its thiol groups [79–81], rendering them not accessible to oxidation by ROS or ii) changing mitochondria from the orthodox to condensed configuration, an alteration that may protect thiol groups of membrane proteins against oxidation. This aspect is in agreement with the observation that ROS, while readily reacting with and damaging vital cellular structures, among them lipids, DNA, and proteins [81], can also regulate protein function thorough modification of specific thiol(s). Over recent years, an increasing number of proteins have been identified that are
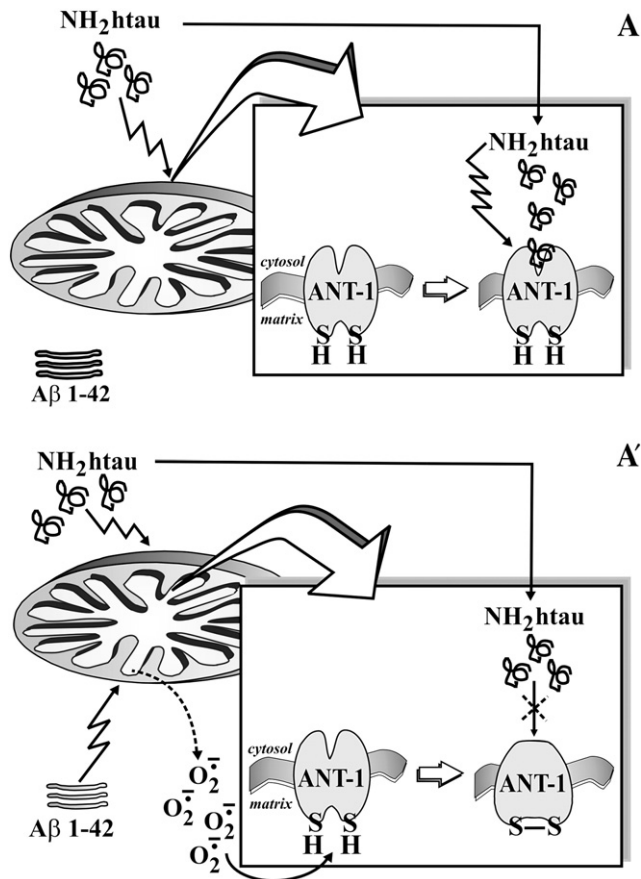
Scheme 1. The molecular mechanism underlying the pathological Aβ-NH$_2$htau interplay on ANT-1 in AD involves thiol group/s present at the active site and the Aβ1-42-induced ROS increase which can oxidize these –SH residues. A: NH$_2$htau fragment affects ANT-1 under conditions in which no interplay with Aβ occurs. A′: NH$_2$htau fragment affects ANT-1 under conditions in which Aβ induced-ROS production oxidizes ANT-1 thiol/s thus modulating NH$_2$htau toxicity. See Discussion for details.

not damaged by oxidative stress conditions but use ROS-mediated thiol modifications to specifically regulate their function [81].

Moreover, although the tau and Aβ pathologies are traditionally considered as harbingers of neuronal damage in AD, we cannot absolutely exclude an alternative, opposite interpretation that these neurological lesions might be generated as a compensatory response by neurons to attenuate this stress, thus representing an important survival response [82–86]. It has been hypothesized that the Aβ peptide, in an initial stage, may act as a ROS scavenger, with ROS production being only observed in a later stage, possibly generated by aggregated Aβ [71,86]. As a consequence, the pro- *vs* anti-oxidant properties of Aβ and the timing of the aggregation *vs* the ROS production are still greatly debated. Anyway during the preparation of this manuscript, Müller's group has shown that mitochondrion-derived ROS result in enhanced amyloidogenic amyloid precursor protein processing, and that Aβ itself leads to mitochondrial dysfunction and increased ROS levels, proposing that starting from mitochondrial dysfunction a vicious cycle is triggered that contributes to the pathogenesis of sporadic AD [87].

5. Conclusions

The picture emerging from this and previous papers is that the molecular mechanism underlying the pathological Aβ-NH$_2$htau interplay on ANT-1 in AD neurons involves i) thiol groups present at the active site [53] and ii) the ROS increase which can oxidize these –SH residues, according to [37].

Aside from that, an important point which requires further consideration here is whether and how NH$_2$htau and Aβ1-42 *functional* interaction could occur *in vivo*; in this regard the time dependence of the peptide formation is crucial. Literature data report that the neurofibrillary tangles appear long after the formation of Aβ plaques, but the neuropathological connection between these two lesions is still not clear [88]. An initial step in the pathogenesis may be the intracellular effect of soluble Aβ on soluble not phosphorylated tau, thus promoting tau phosphorylation and aggregation into PHF-like filaments as well as Aβ nucleation [89–92]. But, interestingly, evidence has been provided that tau is essential for Aβ-induced neurotoxicity [83,93,94], reducing endogenous tau ameliorates amyloid beta-induced deficits in AD mice [94] and Tau-knockout mice exposed to Aβ peptide do not die [95]. Furthermore, it has also been indicated that upon neuron death, monomeric tau becomes an extracellular protein that could be toxic for the surrounding neurons [96]. Thus, if Aβ is already present when the tau fragment is still lacking, it decreases the NH$_2$htau effectiveness on ANT-1 function in a ROS-dependent way, as our data suggest, assuming that Aβ dependent ROS increase acts as modulator/blocker of tau fragment toxicity.

In this context, although, the relative contribution of tau and Aβ remained unclear – as did possible synergistic effects – the pathological convergence between tau and Aβ on AD mitochondria may help to explain why the diseased Aβ- or tau-modifying strategies have not given promising results individually and suggest potential, new pathway(s) and target(s) for a more efficient combined therapeutic intervention of early dysfunction in AD. In addition, the crucial role of ANT-1 impairment in AD onset/progression opens a window for new therapeutic strategies aimed to preserve/ameliorate mitochondrial function and represents an exciting challenge for biochemists. Therefore, besides the treatment and/or removal of both pathological Aβ and tau as well blocking the sites where Aβ initially binds to tau fragment, strategies to protect cells at the mitochondrial level by stabilizing or restoring mitochondrial function or by interfering with the energy metabolism appear to be promising in treating or preventing AD.

References

[1] D.J. Selkoe, Alzheimer's disease is a synaptic failure, Science 298 (2002) 789–791.
[2] G.E. Gibson, H.M. Huang, Oxidative processes in the brain and non-neuronal tissues as biomarkers of Alzheimer's disease, Front. Biosci. 7 (2002) d1007–d1015.
[3] P.I. Moreira, M.S. Santos, C.R. Oliveira, Alzheimer's disease: a lesson from mitochondrial dysfunction, Antioxid. Redox Signal. 9 (2007) 1621–1630.
[4] P.I. Moreira, M.S. Santos, C.R. Oliveira, J.C. Shenk, A. Nunomura, M.A. Smith, X. Zhu, G. Perry, Alzheimer disease and the role of free radicals in the pathogenesis of the disease, Curr. Drug Targets CNS Neurol. Disord. 7 (2008) 3–10.
[5] A. Eckert, S. Hauptmann, I. Scherping, V. Rhein, F. Muller-Spahn, J. Götz, W.E. Muller, Soluble beta-amyloid leads to mitochondrial defects in amyloid precursor protein and tau transgenic mice, Neurodegener. Dis. 5 (2008) 157–159.
[6] B. Su, X. Wang, A. Nunomura, P.I. Moreira, H.G. Lee, G. Perry, M.A. Smith, X. Zhu, Oxidative stress signaling in Alzheimer's disease, Curr. Alzheimer Res. 5 (2008) 525–532.
[7] S. Hauptmann, I. Scherping, S. Drose, U. Brandt, K.L. Schulz, M. Jendrach, K. Leuner, A. Eckert, W.E. Muller, Mitochondrial dysfunction: an early event in Alzheimer pathology accumulates with age in AD transgenic mice, Neurobiol. Aging 30 (2009) 1574–1586.
[8] V. Rhein, X. Song, A. Wiesner, L.M. Ittner, G. Baysang, F. Meier, L. Ozmen, H. Bluethmann, S. Dröse, U. Brandt, E. Savaskan, F. Muller-Spahn, C. Czech, J. Götz, A. Eckert, Amyloid-beta and tau synergistically impair the oxidative phosphorylation system in triple transgenic Alzheimer's disease mice, Proc. Natl. Acad. Sci. U. S. A. 106 (2009) 20057–20062.

[9] S. Sorbi, E.D. Bird, J.P. Blass, Decreased pyruvate dehydrogenase complex activity in Huntington and Alzheimer brain, Ann. Neurol. 1983 (13) (1983) 72–78.

[10] J.P. Blass, Cerebrometabolic abnormalities in Alzheimer's disease, Neurol. Res. 25 (2003) 556–566.

[11] S.M. Cardoso, M.T. Proenca, S. Santos, I. Santana, C.R. Oliveira, Cytochrome c oxidase is decreased in Alzheimer's disease platelets, Neurobiol. Aging 25 (2004) 105–110.

[12] J.L. Chou, D.V. Shenoy, N. Thomas, P.K. Choudhary, F.M. Laferla, S.R. Goodman, G.A. Breen, Early dysregulation of the mitochondrial proteome in a mouse model of Alzheimer's disease, J. Proteomics 74 (2011) 466–479.

[13] P.H. Reddy, M.F. Beal, Amyloid beta, mitochondrial dysfunction and synaptic damage: implications for cognitive decline in aging and Alzheimer's disease, Trends Mol. Med. 14 (2008) 45–53.

[14] S.W. Scheff, D.A. Price, Alzheimer's disease-related alterations in synaptic density: neocortex and hippocampus, J. Alzheimers Dis. 9 (2006) 101–115.

[15] J. Yao, R.W. Irwin, L. Zhao, J. Nilsen, R.T. Hamilton, R.D. Brinton, Mitochondrial bioenergetic deficit precedes Alzheimer's pathology in female mouse model of Alzheimer's disease, Proc. Natl. Acad. Sci. U. S. A. 106 (2009) 14670–14675.

[16] G. Amadoro, M.T. Ciotti, M. Costanzi, V. Cestari, P. Calissano, N. Canu, NMDA receptor mediates tau-induced neurotoxicity by calpain and ERK/MAPK activation, Proc. Natl. Acad. Sci. U. S. A. 103 (2006) 2892–2897.

[17] A. Atlante, G. Amadoro, A. Bobba, L. de Bari, V. Corsetti, G. Pappalardo, E. Marra, P. Calissano, S. Passarella, A peptide containing residues 26–44 of tau protein impairs mitochondrial oxidative phosphorylation acting at the level of the adenine nucleotide translocator, Biochim. Biophys. Acta 1777 (2008) 1289–1300.

[18] G. Amadoro, V. Corsetti, A. Atlante, F. Florenzano, S. Capsoni, R. Bussani, D. Mercanti, P. Calissano, Interaction between NH(2)-tau fragment and Aβ in Alzheimer's disease mitochondria contributes to the synaptic deterioration, Neurobiol. Aging 33 (833) (2012), (e1-833.e25).

[19] A. Fonyo´, SH-group reagents as tools in the study of mitochondrial anion transport, J. Bioenerg. Biomembr. 10 (1978) 171–194.

[20] G. Levi, F. Aloisi, M.T. Ciotti, V. Gallo, Autoradiographic localization and depolarization-induced release of acidic amino acids in differentiating cerebellar granule cell cultures, Brain Res. 290 (1984) 77–86.

[21] A. Atlante, A. Bobba, L. de Bari, F. Fontana, P. Calissano, E. Marra, S. Passarella, Caspase-dependent alteration of the ADP/ATP translocator triggers the mitochondrial permeability transition which is not required for the low-potassium-dependent apoptosis of cerebellar granule cells, J. Neurochem. 97 (2006) 1166–1181.

[22] W.J. Waddell, C. Hill, A simple ultraviolet spectrophotometric method for the determination of protein, J. Lab. Clin. Med. 48 (1956) 311–314.

[23] A. Atlante, S. Passarella, Detection of reactive oxygen species in primary cultures of cerebellar granule cells, Brain Res. Brain Res. Protocol. 4 (1999) 266–270.

[24] H.J. Foman, I. Fridovich, Superoxide dismutase: a comparison of rate constants, Arch. Biochem. Biophys. 158 (1973) 396–400.

[25] K.M. Robinson, M.S. Janes, M. Pehar, J.S. Monette, M.F. Ross, T.M. Hagen, M.P. Murphy, J.S. Beckman, Selective fluorescent imaging of superoxide in vivo using ethidium-based probes, Proc. Natl. Acad. Sci. U. S. A. 103 (2006) 15038–15043.

[26] W. Yang, S. Hekimi, A mitochondrial superoxide signal triggers increased longevity in Caenorhabditis elegans, PLoS Biol. 8 (2010) e1000556, http://dx.doi.org/10.1371/journal.pbio.1000556.

[27] C. Batandier, B. Guigas, D. Detaille, M.Y. El-Mir, E. Fontaine, M. Rigoulet, X.M. Leverve, The ROS production induced by a reverse-electron flux at respiratory-chain complex 1 is hampered by metformin, J. Bioenerg. Biomembr. 38 (2006) 33–42.

[28] V.G. Grivennikova, A.D. Vinogradov, Generation of superoxide by the mitochondrial Complex I, Biochim. Biophys. Acta 1757 (2006) 553–561.

[29] V. Adam-Vizi, C. Chinopoulos, Bioenergetics and the formation of mitochondrial reactive oxygen species, Trends Pharmacol. Sci. 27 (2006) 639–645.

[30] A. Heinen, M. Aldakkak, D.F. Stowe, S.S. Rhodes, M.L. Riess, S.G. Varadarajan, A.K. Camara, Reverse electron flow-induced ROS production is attenuated by activation of mitochondrial Ca^{2+}-sensitive K^+ channels, Am. J. Physiol. Heart Circ. Physiol. 293 (2007) H1400–H1407.

[31] E. Majima, K. Ikawa, M. Takeda, M. Hashimoto, Y. Shinohara, H. Terada, Translocation of loops regulates transport activity of mitochondrial ADP/ATP carrier deduced from formation of a specific intermolecular disulfide bridge catalyzed by copper-o-phenanthroline, J. Biol. Chem. 270 (1995) 29548–29554.

[32] A.E. Vercesi, A.J. Kowaltowski, M.T. Grijalba, A.R. Meinicke, R.F. Castilho, The role of reactive oxygen species in mitochondrial permeability transition, Biosci. Rep. 17 (1997) 43–52.

[33] A.P. Halestrap, K.Y. Woodfield, C.P. Connern, Oxidative stress, thiol reagents, and membrane potential modulate the mitochondrial permeability transition by affecting nucleotide binding to the adenine nucleotide translocase, J. Biol. Chem. 272 (1997) 3346–3354.

[34] L.I. Leichert, F. Gehrke, H.V. Gudiseva, T. Blackwell, M. Ilbert, A.K. Walker, J.R. Strahler, P.C. Andrews, U. Jakob, Quantifying changes in the thiol redox proteome upon oxidative stress in vivo, Proc. Natl. Acad. Sci. U. S. A. 105 (2008) 8197–8202.

[35] R.J.A. Wanders, A.K. Groen, C.W.T. Van Roermund, J.M. Ager, Factors determining the relative contribution of the adeninenucleotide translocator and the ADP-regenerating system to the control of oxidative phosphorylation in isolated rat-liver mitochondria, Eur. J. Biochem. 142 (1984) 417–424.

[36] S. Passarella, A. Atlante, D. Valenti, L. de Bari, The role of mitochondrial transport in energy metabolism, Mitochondrion 2 (2003) 319–343.

[37] A. Atlante, S. Passarella, E. Quagliariello, G. Moreno, C. Salet, Carrier thiols are targets of Photofrin II photosensitization of isolated rat liver mitochondria, J. Photochem. Photobiol. B 7 (1990) 21–32.

[38] A. Atlante, A. Bobba, P. Calissano, S. Passarella, E. Marra, The apoptosis/necrosis transition in cerebellar granule cells depends on the mutual relationship of the antioxidant and the proteolytic systems which regulate ROS production and cytochrome c release en route to death, J. Neurochem. 84 (2003) 960–971.

[39] A. Atlante, L. de Bari, A. Bobba, E. Marra, P. Calissano, S. Passarella, Cytochrome c, released from cerebellar granule cells undergoing apoptosis or excitotoxic death, can generate protonmotive force and drive ATP synthesis in isolated mitochondria, J. Neurochem. 86 (2003) 591–604.

[40] P. Bénit, S. Goncalves, E. Philippe Dassa, J.J. Brière, G. Martin, P. Rustin, Three spectrophotometric assays for the measurement of the five respiratory chain complexes in minuscule biological samples, Clin. Chim. Acta 374 (2006) 81–86.

[41] H. Atamna, W.H. Frey II, Mechanisms of mitochondrial dysfunction and energy deficiency in Alzheimer's disease, Mitochondrion 7 (2007) 297–310.

[42] X. Wang, B. Su, H. Fujioka, X. Zhu, Dynamin-like protein 1 reduction underlies mitochondrial morphology and distribution abnormalities in fibroblasts from sporadic Alzheimer's disease patients, Am. J. Pathol. 173 (2008) 470–482.

[43] M.J. Calkins, M. Manczak, P. Mao, U. Shirendeb, P.H. Reddy, Impaired mitochondrial biogenesis, defective axonal transport of mitochondria, abnormal mitochondrial dynamics and synaptic degeneration in a mouse model of Alzheimer's disease, Hum. Mol. Genet. 20 (2011) 4515–4529.

[44] E. Cadenas, K.J. Davies, Mitochondrial free radical generation, oxidative stress, and aging, Free Radic. Biol. Med. 29 (2000) 222–230.

[45] A. Atlante, P. Calissano, A. Bobba, A. Azzariti, E. Marra, S. Passarella, Cytochrome c is released from mitochondria in a reactive oxygen species (ROS)-dependent fashion and can operate as a ROS scavenger and as a respiratory substrate in cerebellar neurons undergoing excitotoxic death, J. Biol. Chem. 275 (2000) 37159–37166.

[46] R.G. Hansford, B.A. Hogue, V. Mildaziene, Dependence of H_2O_2 formation by rat heart mitochondria on substrate availability and donor age, J. Bioenerg. Biomembr. 29 (1997) 89–95.

[47] S.S. Korshunov, V.P. Skulachev, A.A. Starkov, High protonic potential actuates a mechanism of production of reactive oxygen species in mitochondria, FEBS Lett. 416 (1997) 15–18.

[48] Q. Chen, E.J. Vazquez, S. Moghaddas, C.L. Hoppel, E.J. Lesnefsky, Production of reactive oxygen species by mitochondria: central role of complex III, J. Biol. Chem. 278 (2003) 36027–36031.

[49] A. Atlante, L. de Bari, A. Bobba, E. Marra, S. Passarella, Transport and metabolism of L-lactate occur in mitochondria from cerebellar granule cells and are modified in cells undergoing low potassium dependent apoptosis, Biochim. Biophys. Acta 1767 (2007) 1285–1299.

[50] A. Atlante, S. Gagliardi, E. Marra, P. Calissano, S. Passarella, Glutamate neurotoxicity in rat cerebellar granule cells involves cytochrome c release from mitochondria and mitochondrial shuttle impairment, J. Neurochem. 73 (1999) 237–246.

[51] A. Eckert, K. Schmitt, J. Götz, Mitochondrial dysfunction — the beginning of the end in Alzheimer's disease? Separate and synergistic modes of tau and amyloid-β toxicity, Alzheimers Res. Ther. 3 (2011) 15.

[52] P. Calissano, C. Matrone, G. Amadoro, Apoptosis and in vitro Alzheimer disease neuronal models, Commun. Integr. Biol. 2 (2009) 163–169.

[53] D. Sepulveda-Falla, J. Matschke, C. Bernreuther, C. Hagel, B. Puig, A. Villegas, G. Garcia, J. Zea, B. Gomez-Mancilla, I. Ferrer, F. Lopera, M. Glatzel, Deposition of hyperphosphorylated tau in cerebellum of PS1 E280A Alzheimer's disease, Brain Pathol. 21 (2011) 452–463.

[54] J. Kuan, M.H. Saier Jr., The mitochondrial carrier family of transport proteins: structural, functional, and evolutionary relationships, Crit. Rev. Biochem. Mol. Biol. 28 (1993) 209–233.

[55] A.J. Kowaltowski, A.E. Vercesi, R.F. Castilho, Mitochondrial membrane protein thiol reactivity with N-ethylmaleimide or mersalyl is modified by Ca^{2+}: correlation with mitochondrial permeability transition, Biochim. Biophys. Acta 1318 (1997) 395–402.

[56] G. McStay, S.J. Clarke, A.P. Halestrap, Role of critical thiol groups on the matrix surface of the adenine nucleotide translocase in the mechanism of the mitochondrial permeability transition pore, Biochem. J. 367 (2002) 541–548.

[57] N. Brustovetsky, M. Klingenberg, The reconstituted ADP/ATP carrier can mediate H^+ transport by free fatty acids, which is further stimulated by mersalyl, J. Biol. Chem. 269 (1994) 27329–27336.

[58] E. Majima, H. Koike, Y.M. Hong, Y. Shinohara, H. Terada, Characterization of cysteine residues of mitochondrial ADP/ATP carrier with the SH-reagents eosin 5-maleimide and N-ethylmaleimide, J. Biol. Chem. 268 (1993) 22181–22187.

[59] M. Klingenberg, The ADP and ATP transport in mitochondria and its carrier, Biochem. Biophys. Acta 1778 (2008) 1978–2021.

[60] J.R. Aprille, G.K. Asimakis, Postnatal development of rat liver mitochondria: state 3 respiration, adenine nucleotide translocase activity, and the net accumulation of adenine nucleotides, Arch. Biochem. Biophys. 201 (1980) 564–575.

[61] J. Austin, J.R. Aprille, Carboxyatractyloside-insensitive influx and efflux of adenine nucleotides in rat liver mitochondria, J. Biol. Chem. 259 (1984) 154–160.

[62] J.K. Pollak, R. Sutton, The differentiation of animal mitochondria during development, Trends Biochem. Sci. 5 (1980) 23–27.

[63] C. Fiore, V. Trezeguet, A. Le Saux, P. Roux, C. Schwimmer, A.C. Dianoux, F. Noel, G.J. Lauquin, G. Brandolin, P.V. Vignais, The mitochondrial ADP/ATP carrier: structural, physiological and pathological aspects, Biochimie 80 (1998) 137–150.

[64] M. Le Bras, M.V. Clément, S. Pervaiz, C. Brenner, Reactive oxygen species and the mitochondrial signaling pathway of cell death, Histol. Histopathol. 20 (2005) 205–219.

[65] G. Moreno, G. Poussin, F. Ricchelli, C. Salet, The effects of singlet oxygen produced by photodynamic action on the mitochondrial permeability transition differ in accordance with the localization of the sensitizer, Arch. Biochem. Biophys. 386 (2001) 243–250.

[66] A. Atlante, S. Passarella, E. Quagliariello, G. Moreno, C. Salet, Haematoporphyrin derivative (Photofrin II) photosensitization of isolated mitochondria: inhibition of ADP/ATP translocator, J. Photochem. Photobiol. B 4 (1989) 35–46.

[67] D.A. Butterfield, Amyloid beta-peptide (1-42)-induced oxidative stress and neurotoxicity: implications for neurodegeneration in Alzheimer's disease brain. A review, Free Radic. Res. 36 (2002) 1307–1313.

[68] R. Naylor, A.F. Hill, K.J. Barnham, Neurotoxicity in Alzheimer's disease: is covalently crosslinked A_beta responsible? Eur. Biophys. J. 37 (2008) 265–268.

[69] K.J. Barnham, G.D. Ciccotosto, A.K. Tickler, F.E. Ali, D.G. Smith, N.A. Williamson, Y.H. Lam, D. Carrington, D. Tew, G. Kocak, I. Volitakis, F. Separovic, C.J. Barrow, J.D. Wade, C.L. Masters, R.A. Cherny, C.C. Curtain, A.I. Bush, R. Cappai, Neurotoxic, redox-competent Alzheimer's beta-amyloid is released from lipid membrane by methionine oxidation, J. Biol. Chem. 278 (2003) 42959–42965.

[70] M.S. Lustgarten, A. Bhattacharya, F.L. Muller, Y.C. Jang, T. Shimizu, T. Shirasawa, A. Richardson, H. Van Remmen, Complex I generated, mitochondrial matrix-directed superoxide is released from the mitochondria through voltage dependent anion channels, Biochem. Biophys. Res. Commun. 422 (2012) 515–521.

[71] R.S. Balaban, S. Nemoto, T. Finkel, Mitochondria, oxidants, and aging, Cell 120 (2005) 483–495.

[72] J. Park, J. Lee, C. Choi, Mitochondrial network determines intracellular ROS dynamics and sensitivity to oxidative stress through switching inter-mitochondrial messengers, PLoS One 6 (2011) 3211.

[73] T.V. Votyakova, I.J. Reynolds, $\Delta\Psi$-Dependent and -independent production of reactive oxygen species by rat brain mitochondria, J. Neurochem. 79 (2001) 266–277.

[74] T.R. Hurd, T.A. Prime, M.E. Harbour, K.S. Lilley, M.P. Murphy, Detection of reactive oxygen species-sensitive thiol proteins by redox difference gel electrophoresis: implications for mitochondrial redox signaling, J. Biol. Chem. 282 (2007) 22040–22051.

[75] T.S. Chang, C.S. Cho, S. Park, S. Yu, S.W. Kang, S.G. Rhee, Peroxiredoxin III, a mitochondrion-specific peroxidase, regulates apoptotic signaling by mitochondria, J. Biol. Chem. 279 (2004) 41975–41984.

[76] I.S. Kil, J.W. Park, Regulation of mitochondrial NADP$^+$-dependent isocitrate dehydrogenase activity by glutathionylation, J. Biol. Chem. 280 (2005) 10846–10854.

[77] C.C. Dahm, K. Moore, M.P. Murphy, Persistent S-nitrosation of complex I and other mitochondrial membrane proteins by S-nitrosothiols but not nitric oxide or peroxynitrite: implications for the interaction of nitric oxide with mitochondria, J. Biol. Chem. 281 (2006) 10056–10065.

[78] E.R. Taylor, F. Hurrell, R.J. Shannon, T.K. Lin, J. Hirst, M.P. Murphy, Reversible glutathionylation of complex I increases mitochondrial superoxide formation, J. Biol. Chem. 278 (2003) 19603–19610.

[79] M. Klingenberg, Molecular aspects of the adenine nucleotide carrier from mitochondria, Arch. Biochem. Biophys. 270 (1989) 1–14.

[80] E. Majima, Y. Shinohara, N. Yamaguchi, Y. Hong, H. Terada, Importance of loops of mitochondrial ADP/ATP carrier for its transport activity deduced from reactivities of its cysteine residues with the sulfhydryl reagent eosin-5-maleimide, Biochemistry 33 (1994) 9530–9536.

[81] P.V. Vignais, P.M. Vignais, Effect of SH reagents on atractyloside binding to mitochondria and ADP translocation. Potentiation by ADP and its prevention by uncoupler FCCP, FEBS Lett. 26 (1972) 27–31.

[82] M.A. Smith, J.A. Joseph, G. Perry, Arson: tracking the culprit in Alzheimer's disease, Ann. N. Y. Acad. Sci. 924 (2000) 35–38.

[83] M.A. Smith, C.S. Atwood, J.A. Joseph, G. Perry, Predicting the failure of the amyloid-beta vaccine, Lancet 359 (2002) 1864–1865.

[84] J. Joseph, B. Shukitt-Hale, N.A. Denisova, A. Martin, G. Perry, M.A. Smith, Copernicus revisited: amyloid beta in Alzheimer's disease, Neurobiol. Aging 22 (2001) 131–146.

[85] C.A. Rottkamp, C.S. Atwood, J.A. Joseph, A. Nunomura, G. Perry, M.A. Smith, The state *versus* amyloid-β: the trial of the most wanted criminal in Alzheimer disease, Peptides 23 (2002) 1333–1341.

[86] C. Hureau, P. Faller, Abeta-mediated ROS production by Cu ions: structural insights, mechanisms and relevance to Alzheimer's disease, Biochimie 91 (2009) 1212–1217.

[87] K. Leuner, T. Schütt, C. Kurz, S.H. Eckert, C. Schiller, A. Occhipinti, S. Mai, M. Jendrach, G.P. Eckert, S.E. Kruse, R.D. Palmiter, U. Brandt, S. Dröse, I. Wittig, M. Willem, C. Haass, A.S. Reichert, W.E. Müller, Mitochondrion-derived reactive oxygen species lead to enhanced amyloid beta formation, Antioxid. Redox Signal. 16 (2012) 1421–1433.

[88] J.A. Fein, S. Sokolow, C.A. Miller, H.V. Vinters, F. Yang, G.M. Cole, K.H. Gylys, Co-localization of amyloid beta and tau pathology in Alzheimer's disease synaptosomes, Am. J. Pathol. 172 (2008) 1683–1692.

[89] J. Busciglio, A. Lorenzo, J. Yeh, B.A. Yankner, βeta-amyloid fibrils induce tau phosphorylation and loss of microtubule binding, Neuron 14 (1995) 879–888.

[90] W.H. Zheng, S. Bastianetto, F. Mennicken, W. Ma, S. Kar, Amyloid beta peptide induces tau phosphorylation and loss of cholinergic neurons in rat primary septal cultures, J. Neurosci. 115 (2002) 201–211.

[91] K.B. Rank, A.M. Pauley, K. Bhattacharya, Z. Wang, D.B. Evans, T. Fleck, J.A. Johnston, S.K. Sharma, Direct interaction of soluble human recombinant Abeta 1-42 results in tau aggregation and hyperphosphorylation by tau protein kinase II, FEBS Lett. 514 (2002) 263–268.

[92] J.P. Guo, T. Arai, J. Miklossy, P.L. McGeer, Abeta and tau form soluble complexes that may promote self aggregation of both into the insoluble forms observed in Alzheimer's disease, Proc. Natl. Acad. Sci. U. S. A. 103 (2006) 1953–1958.

[93] M. Rapoport, H.N. Dawson, L.I. Binder, M.P. Vitek, A. Ferreira, Tau is essential for beta-amyloid-induced neurotoxicity, Proc. Natl. Acad. Sci. U. S. A. 99 (2002) 6364–6369.

[94] E.D. Roberson, K. Scearce-Levie, J.J. Palop, F. Yan, I.H. Cheng, T. Wu, H. Gerstein, G.Q. Yu, L. Mucke, Reducing endogenous tau ameliorates amyloid beta-induced deficits in an Alzheimer's disease mouse model, Science 316 (2007) 750–754.

[95] H.N. Dawson, A. Ferreira, M.V. Eyster, N. Ghoshal, L.I. Binder, M.P. Vitek, Inhibition of neuronal maturation in primary hippocampal neurons from tau deficient mice, J. Cell Sci. 114 (2001) 1179–1187.

[96] A. Gómez-Ramos, M. Díaz-Hernández, R. Cuadros, F. Hernández, J. Avila, Extracellular tau is toxic to neuronal cells, FEBS Lett. 580 (2006) 4842–4850.